Eur Biophys J (2009) 38:219–228
DOI 10.1007/s00249-008-0373-1

ORIGINAL PAPER

Pressure jump relaxation investigations of lipid membranes using FTIR spectroscopy

Martin Schiewek · Alfred Blume

Received: 30 May 2008 / Revised: 29 July 2008 / Accepted: 4 August 2008 / Published online: 2 October 2008

Abstract The relaxation kinetics of aqueous lipid dispersions after a pressure jump (p-jump) were investigated using time-resolved FTIR spectroscopy. The methylene stretching vibrational band and the carbonyl band were analyzed to detect changes in conformational order of the hydrocarbon chains and to follow the degree of hydration of the head group, respectively. The kinetics of the transition was found to consist of multiple processes with relaxation constants from seconds down to milliseconds. Faster processes are also present, but could not be resolved by our instrument. This is the first investigation showing directly the time resolved change in chain order in lipid bilayers induced by a p-jump. The results obtained with this IR detection method support previous results that the change in chain order after a perturbation is a multi-step process with the initial molecular events occurring with time constants shorter than milliseconds.

Keywords Pressure jump · Phase transition · Infrared spectroscopy · Kinetics

Abbreviations

DEPC	1,2-Dielaidoyl-*sn*-glycero-3-phosphocholine
DMPA	1,2-Dimyristoyl-*sn*-glycero-3-phosphatidic acid
DMPE	1,2-Dimyristoyl-*sn*-glycero-3-phosphoethanolamine
DOPE	1,2-Dioleoyl-*sn*-glycero-3-phosphoethanolamine
DPPC	1,2-Dipalmitoyl-*sn*-glycero-3-phosphocholine
DSPC	1,2-Distearoyl-*sn*-glycero-3-phosphocholine
FTIR	Fourier transform infrared spectroscopy
SANS	Small angle neutron scattering
T_M	Main transition temperature

M. Schiewek · A. Blume (✉)
Faculty of Chemistry and Physics, Institute of Chemistry,
Martin-Luther-University Halle-Wittenberg,
Mühlpforte 1, 06108 Halle (Saale), Germany
e-mail: alfred.blume@chemie.uni-halle.de

Introduction

Aqueous phospholipid dispersions show a complex lyotropic phase behavior including lamellar, hexagonal and cubic phases. Transitions between different phases can be induced by changing an external parameter like temperature, pressure or concentration. In many cases, these phase transitions are very fast and require the application of relaxation techniques (Eigen 1968), such as a fast change (jump) of an external parameter. The pressure jump (p-jump) technique is a suitable method to investigate the chain-melting transition of lipid systems. This gel–fluid phase transition is very pressure sensitive and shifts by about 22 K/kbar (Winter and Czeslik 2000). Pressure jumps can be easily performed in both directions and with arbitrary amplitudes. The advantage of p-jump experiments is that relaxation times over several orders of magnitude, i.e. in the range of 10^{-3} to 10^{2} s can be observed. The advantage of a temperature jump experiment is that the dead time is much shorter, but the disadvantage is that due to the fast cooling process after the T-jump the longer time scales are not accessible.

Several p-jump investigations on aqueous lipid dispersions using calorimetry (Grabitz et al. 2002), turbidity (Blume and Hillmann 1986; Elamrani and Blume 1983; Gruenewald et al. 1980) or X-ray scattering (Erbes et al. 2000) as a detection method have been reported in the literature before. Interestingly, the interpretation of the results led to different concepts about the processes occurring during the relaxation.

The turbidity measurements showed that the phase transition is characterized by multiple processes having relaxation constants in different time regimes. The results were discussed in terms of nucleation and domain growing steps, similar to the cluster model of Kanehisa and Tsong (1978). The formation of domains of the new phase was assumed to be the rate determining step, which is considerably slowed down at the midpoint temperature of the phase transition.

The group of Winter monitored changes in X-ray and SANS patterns after p-jumps and found that not in all cases the transition can be described by a two-state model. They assumed a third unknown state to be involved in transitions of DEPC. This temporary phase could be monitored after a rapid decay (<5 ms) of the initial phase and cannot be found among the stationary phases in the *p*, *T*-diagram of DEPC. The authors describe that this might also occur during the main transition of DOPE. They conclude that, in most cases, the phase transition kinetics is mainly determined by the transport and reallocation of solvent (water). Nucleation processes are determining the kinetics only in those cases where water reallocation has little influence. In the latter case, the transition is much faster.

A different concept for the phase transition kinetics has been suggested by the group of Heimburg (Grabitz et al. 2002). The sample is described by a large ensemble of highly cooperative sub-systems whose enthalpy is fluctuating due to energy exchange among the systems. When the total system is sufficiently close to the phase transition, a number of sub-systems is already in the opposite phase. Using the fluctuation-dissipation theorem, the authors suggested that the fluctuation time (expressed by the decay constant of the enthalpy correlation function) is very long close to the transition midpoint. A sudden change of an external parameter inducing a change in the degree of transition cannot lead to shorter times than the time specified by the fluctuation time. This theory implies that the transition occurs as a *single* process with one single step only. The relaxation rate can then be simulated using a two-dimensional Ising model. The theory has been tested using calorimetric measurements with a p-jump shifting the phase transition to a different temperature. The results showed that the relaxation time as a function of temperature followed closely the heat capacity curve determined by DSC. Similar results have been reported by Hinz and Coworkers recently (Boehm et al. 2007).

Due to the large discrepancies in the experimental results obtained with different methods, where relaxation time constants were found in the microsecond to the second time regime, we decided to use a method, where information on the order of the molecules could be obtained on the molecular level. We therefore used time resolved FTIR spectroscopy as a new detection method. The CH_2 vibrational bands of the lipid molecules are sensitive to changes in conformational order and the C=O bands is sensitive to hydration (Blume et al. 1988). This differentiates this method from methods like calorimetry or light scattering/turbidity, which are sensitive to macroscopic properties only. Conformational changes of the fatty acid chains during the gel–fluid transition lead to a higher content of gauche conformers and a decrease of the chain order parameter. Concomitantly, the frequency of the symmetric and antisymmetric methylene stretching vibration mode [$\nu_{as}(CH_2)$ and $\nu_s(CH_2)$] shifts to higher values. Furthermore, hydration of the lipid head group region will increase while undergoing the transition. This effect weakens the carbonyl bond due to hydrogen bonding and leads to a decrease of the frequency of the carbonyl stretching vibration mode [ν(C=O)]. Kinetic information on these processes can than be obtained by plotting the frequencies of these modes as a function of time after the perturbation of the system by a p-jump.

Experimental

Lipids were purchased from Genzyme Pharmaceuticals (Cambridge, USA). Before use, they were three times dispersed in D_2O (99.9%, glass distilled, Aldrich, St Louis, USA) and lyophilized to ensure complete H/D exchange. All samples were prepared as multilamellar vesicles (MLV) in D_2O (1.5 wt.%). The sample was heated to 10°C over T_M and vortexed and sonicated until completely hydrated. It was then transferred to IR cell using a syringe. The cell was preheated to 10°C over T_M. This procedure avoids formation of bubbles due to a lowered sample viscosity. In case of DMPA, the sample was prepared with a 100 mM phosphate buffer solution. The deuterated phosphate salts were prepared from conventional potassium salts (Aldrich) by H/D exchange as described above. The *pD* value was adjusted to $pD = 6.0$ using an pH-meter (pMX3000, WTW GmbH, Weilheim, Germany).

FTIR spectra were recorded after a p-jump from 100 bar to ambient pressure using an IFS66s/v spectrometer (Bruker, Ettlingen, Germany). The IR cell, a flow-through cell with MgO windows made by Graceby–Specac (Kent, UK), is pressure resistant up to 300 bars and has a sample thickness of 50 μm. After a p-jump, 500 spectra (8 cm^{-1} resolution) were measured consecutively in one series. The time for the measurement of one single beam spectrum was 8 ms. Therefore, the time resolution of the experiment was determined by the detection system in the rapid scan mode, because the p-jump time was only 4 ms. A series of 82 jumps were averaged to increase the s/n ratio. All single beam sample spectra were corrected by subtraction of one D_2O spectrum measured under identical experimental

conditions at the transition midpoint T_M of the particular lipid. The solvent spectrum was assumed to show no changes over the small measured temperature interval ($\approx$1 K). A detailed description of the instrument and the processing of the spectra can be found in a previous paper (Schiewek et al. 2007).

Results

FTIR Spectra

Normal spectra at high and low pressure were measured to determine the suitable temperature interval for the isothermal kinetic experiments that were carried out immediately afterwards. The phase transition can be monitored by plotting the wavenumber of specific bands, such as the methylene stretching bands, versus temperature. Fig. 1a shows the increase of the wavenumber of the $\nu_s(CH_2)$ vibrational band of DSPC at temperatures around T_M at ambient and at a pressure of 100 bar. The phase transition midpoint temperature T_M is increased by $\approx$2 K by the pressure increase to 100 bar. The data in Fig. 1a were used to calculate the degree of transition θ (plotted in Fig. 1b) according to Eq. 1.

$$\theta = \frac{(\tilde{\nu}^{\text{fluid}} - \tilde{\nu})}{\tilde{\nu}^{\text{fluid}} - \tilde{\nu}^{\text{gel}}} \quad (1)$$

In a time-resolved p-jump experiment, the pressure changes from 100 bar excess pressure to ambient pressure. Therefore, a wavenumber shift can be observed as indicated by the blue arrows in Fig. 1. The transition is considerably slowed down with the relaxation constant τ having the highest value, when the temperature is exactly at the transition midpoint at $\Delta\theta = 0.5$ of the transition curve at ambient pressure (cf. blue arrow and τ-T-function in Fig. 1b). At this temperature, however, the amplitude of the wavenumber shift has only half its maximal value. The investigated temperature intervall ΔT was choosen to be centered around this temperature. To enlarge this interval over the thresholds for ΔT, as drawn in Fig. 1a was not useful, because at lower temperature, the wavenumber shift is close to zero and at higher temperature, the transition kinetics becomes so fast that it cannot be resolved by the instrument.

A set of time resolved spectra of a DSPC sample measured after a p-jump from 100 bar to ambient pressure is shown in Fig. 2. The spectra were corrected by the D_2O absorptions. However, the D_2O spectrum subtraction leads to some artifacts at $\approx$2,750 and $\approx$2,150 cm^{-1} caused by small differences in the ν(O–D) band shape of the D_2O band between pure D_2O and the lipid–water sample. Due to the total absorption occuring in this region, the absorbance values in the spectral range between these two values are artifacts.

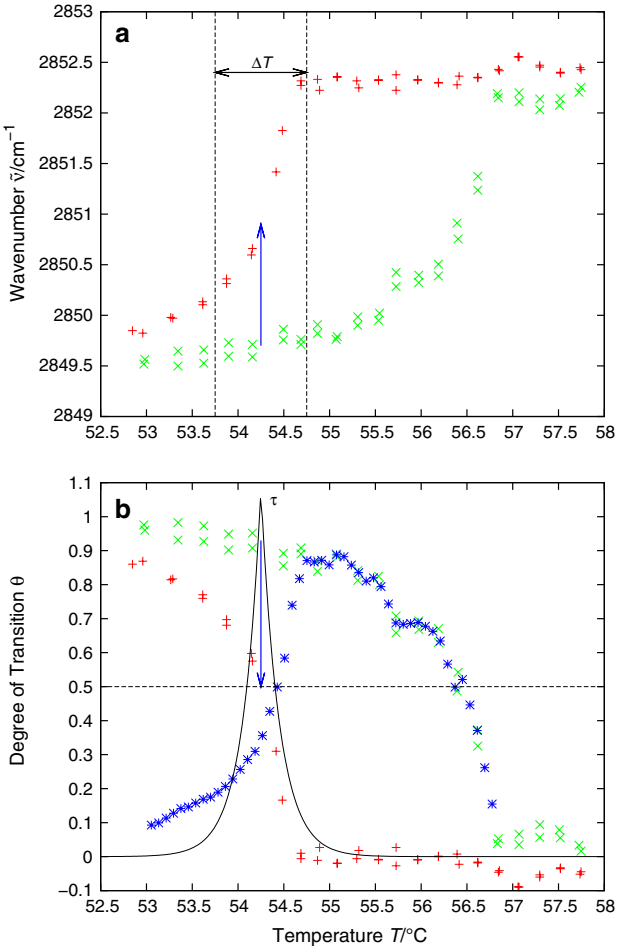

Fig. 1 *Upper plot* Temperature dependence of the wavenumber of the $\nu_s(CH_2)$ band of DSPC at ambient pressure (*plus*) and 100 bar excess pressure (*times*). *Dotted lines* represent the interval ΔT used for time-resolved measurements. *Lower plot* θ-T-curves calculated from the data shown in the upper plot. The difference $\Delta\theta$ (*asterisk*) between both curves were calculated from interpolated and smoothed datasets. *Blue arrows* in both plots represent the amplitude of the wavenumber change or change in θ in a p-jump experiment at a temperature, where the longest relaxation time is expected. The maximum of the τ-T-curve (*solid line*, schematic representation, no axes) is always found at lower temperature compared to the maximum of the $\Delta\theta$-curve

The absorption bands of the spectra before the p-jump have intensities twice as high as those of the posttrigger spectra. This is caused by a larger sample thickness in the pressurized state of the cell which could not be avoided. The inset of Fig. 2 shows the evolution of the $\nu_{as}(CH_2)$ peak maximum as a function of time. The frequency of the band increases by 2 cm^{-1}. This is a small value when compared to the 8 cm^{-1} resolution of the spectra. However, these small shifts can be determined with sufficient precision as long as the peak is broad enough to have an

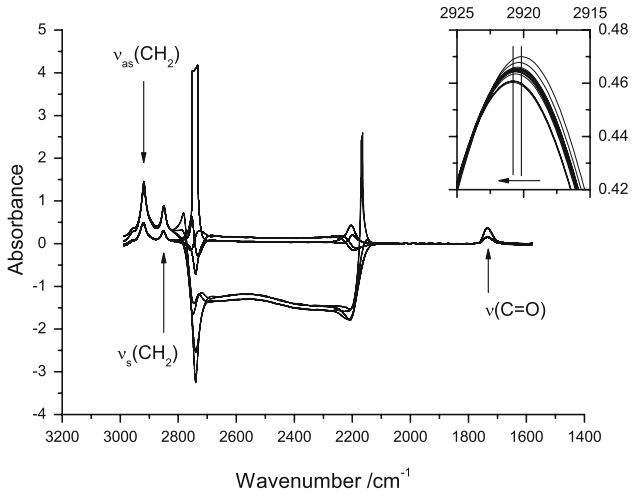

Fig. 2 Evolution of spectra of DSPC before and after a p-jump from 100 bar to ambient pressure at 53.57°C (after subtraction of D_2O spectra). *Inset* $\nu_{as}(CH_2)$ band peak of posttrigger spectra. See text for further information

adequate number of points for the interpolation algorithm (Cameron et al. 1982). Spectra with higher resolution can be obtained, but this would lower the time resolution. Therefore, the current set up of 8 cm^{-1} spectral resolution versus 8 ms time resolution was a compromise. Due to this compromise, information about the complex band structure of the ν(C=O) vibration, for instance, cannot be obtained. This band at 1,740 cm^{-1} is known to consist of at least 2 subpeaks (Blume et al. 1988). Furthermore, this band is strongly disturbed by noise due to the broad (D_2O) association band of the solvent having its maximum at 1,555 cm^{-1}. As a consequence, only limited information about carbonyl group hydration can be obtained from the analysis of the C=O band. The spectra of DSPC in Fig. 2 are shown as an example representing all other lipid spectra in this paper. All other lipid spectra look very similar and will not be shown.

Kinetic traces

General remarks on data fitting

The traces of wavenumber versus time were fitted using a multiexponential model:

$$\tilde{\nu}(t) = \tilde{\nu}_0 + \sum_{i=1}^{j} \Delta\tilde{\nu}_i[1 - \exp(-t/\tau_i)] \quad \tau_i < \tau_{i+1}. \tag{2}$$

The starting wavenumber $\tilde{\nu}_0$ in Eq. 2 was determined by averaging the wavenumber of the position of all pretrigger spectra, this value was fixed and not varied by the fitting algorithm. The relaxation constant τ_1 represents the observed fast process that could not be resolved due to the instrumental dead time of ca. 8 ms, it was arbitrarily fixed to 1 ms. The number of exponential terms j was determined before fitting taking into account the s/n-ratio and the "visibility" of several processes as judged by eye. In most cases, three terms were used to obtain a reasonable fit. This is possible, because the spacing and the number of wavenumber points is sufficient to three orders of magnitude in time. The use of a higher numbers of exponential terms ($j > 3$) would lead to lower values of χ^2. However, due to the considerable noise in the wavenumber versus time curves, the use of a sum of exponentials with time constants differing less than a factor of five is not justified.

Boundary conditions were introduced to keep all τ_i values distinguishable in an increasing order. The determination of the amplitudes (wavenumber shifts) $\Delta\tilde{\nu}_i$ for the different processes is reliable. Care must be taken for the determination of small values of τ_i, which are close to the time resolution of the instrument, or large values of τ_i, which are close to or larger than the measured time interval. Furthermore, a correct determination of the time constants breaks down when the amplitude and the noise level of the trace are of the same order of magnitude.

DSPC

Kinetic traces of the $\nu_{as}(CH_2)$, $\nu_s(CH_2)$ and ν(C=O) vibration modes are plotted in Fig. 3a–c. All traces have in common that the pretrigger points are highly influenced by noise due to the increased sample thickness at 100 bar when the cell is still under pressure (see Sect. 3.1). After the pressure jump from 100 bar excess pressure to ambient pressure, the wavenumber of the methylene stretching vibrations shifts to higher values. The maximum of the ν(C=O) band decreases to lower wavenumbers. The main part of the shift belongs to processes that cannot be resolved by the instrument. Slow processes are visible, but have only small amplitudes (wavenumber shifts).

The temperature dependencies of the amplitudes $\Delta\tilde{\nu}_i$ (Fig. 3d–f) and relaxation constants τ_i (Fig. 3g–i) look very similar for the $\nu_{as}(CH_2)$ and $\nu_s(CH_2)$ vibration. $\Delta\tilde{\nu}_1$ is still rising with increasing temperature, while $\Delta\tilde{\nu}_2$ and $\Delta\tilde{\nu}_3$ are going throug a maximum at 54.28 and 54.17°C, respectively. Generally, the wavenumber shifts of the slower processes are smaller than those belonging to the faster ones.

The sum of all $\Delta\tilde{\nu}_i$ represents the difference between the two stationary, time-independent values $\tilde{\nu}^{0\ bar}(T)$ and $\tilde{\nu}^{100\ bar}(T)$. The maximum of the wavenumber shift is expected to occur half-way between $T_M^{100\ bar}$ (55.7°C) and $T_M^{0\ bar}$ (53.55°C). It can be seen in Fig. 3d–f, that the maxima of the $\sum\Delta\tilde{\nu}_i$ curves for each vibration mode is outside of the measured temperature interval. The amplitude maximum of each individual process shifts to lower temperatures for the slower processes. The same behavior can be found for the ν(C=O) wavenumber shift.

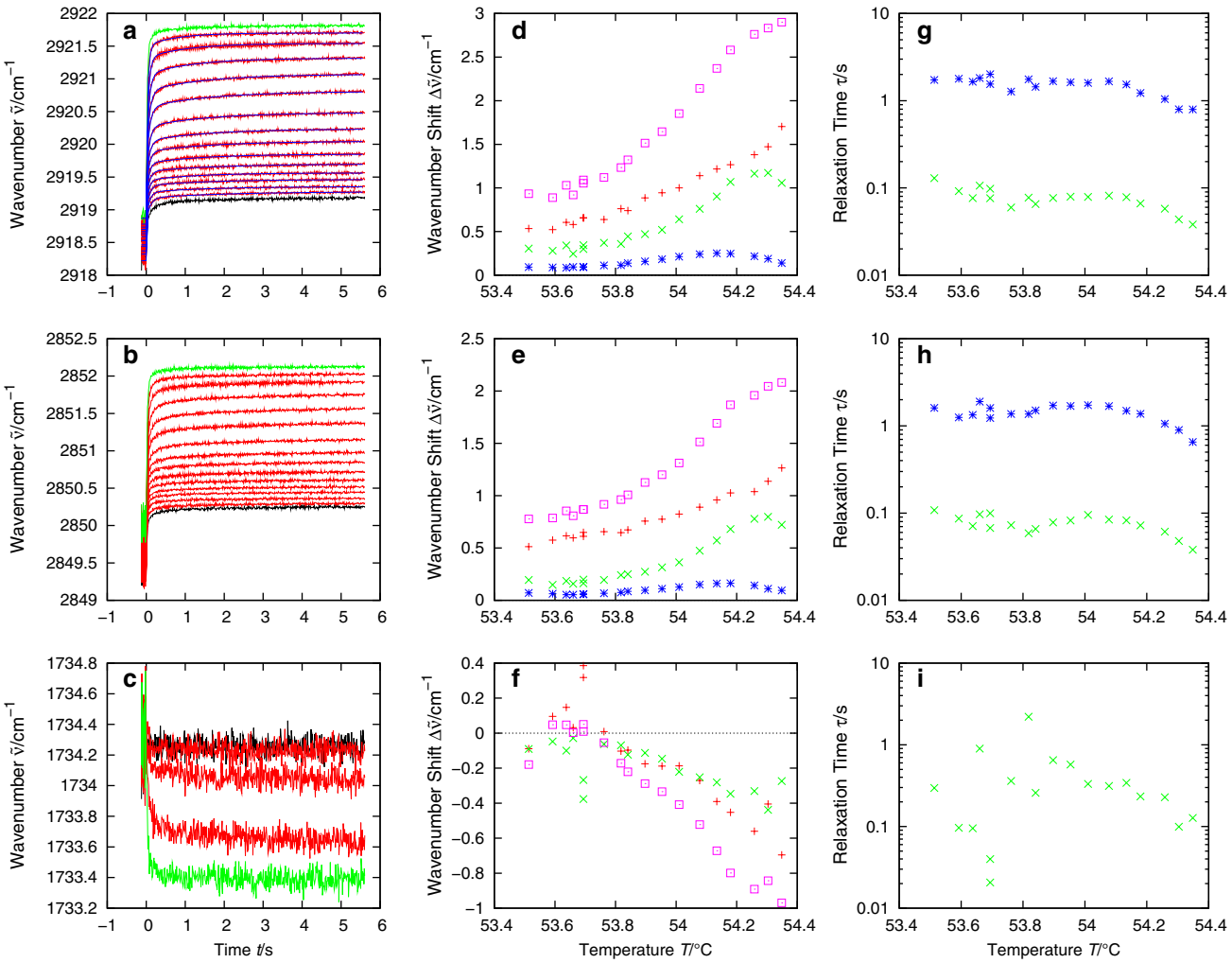

Fig. 3 *Left column* Selection of p-jump traces of the $\nu_{as}(CH_2)$, $\nu_s(CH_2)$ and ν(C=O) peak (**a**, **b**, **c**) of DSPC in a temperature interval from 53.51°C (*black line*) to 54.35°C (*green line*). Fit results according to Eq. 2 are shown for the $\nu_{as}(CH_2)$ trace (*blue line*). *Middle column* Amplitudes (**d**, **e**, **f**) $\Delta\tilde{\nu}_1$ (*plus*), $\Delta\tilde{\nu}_2$ (*times*), $\Delta\tilde{\nu}_3$ (*asterisk*), sum of $\Delta\tilde{\nu}_i$ (*square*). *Right column* Relaxation times (**g**, **h**, **i**) τ_2 (*times*), τ_3 (*asterisk*)

Due to the low s/n-ratio, these traces were fitted using only a 2-term exponential function.

The relaxation constants τ_2 and τ_3 of the methylene stretching vibration traces are shown in Fig. 3g, h. Each curve shows a maximum at ca. 54°C, the main transition midpoint temperature at ambient pressure (T_M^{0bar}). At temperatures below 53.8°C, the τ_i values are not very reliable, because the determination of the values is difficult due to the small amplitude values (wavenumber shifts) in this temperature region. The same problem occurs for the time constant data derived from the ν(C=O) vibration band shown in Fig. 3i. Despite the noise, a maximum seems to be present at the same temperature at ca. 54°C. The time constant for the slowest process with the smallest amplitude is in the s time regime, whereas the second faster process with a slightly larger amplitude is in the 50–200 ms regime. The fastest not resolvable process has the largest amplitude. From these results, it is apparent that the transition process is a multi-step process with two steps which can be resolved by the IR-method and at least one faster process with a time constant below 8 ms.

DPPC

Kinetic traces of the methylene stretching vibrations of a DPPC sample are shown in Fig. 4a, b. The traces obtained for the carbonyl vibration have a noise level that is too high for a determination of relaxation constants and are, therefore, not shown. The wavenumber of the methylene stretching vibrations increases rapidly after a p-jump, but in contrast to the corresponding traces observed for DSPC (Fig. 3a–c), a small decrease in wavenumger is seen on a longer time scale. In most cases, this decrease is very close to being linear. Apparently, this decrease is an instrumental artifact, which

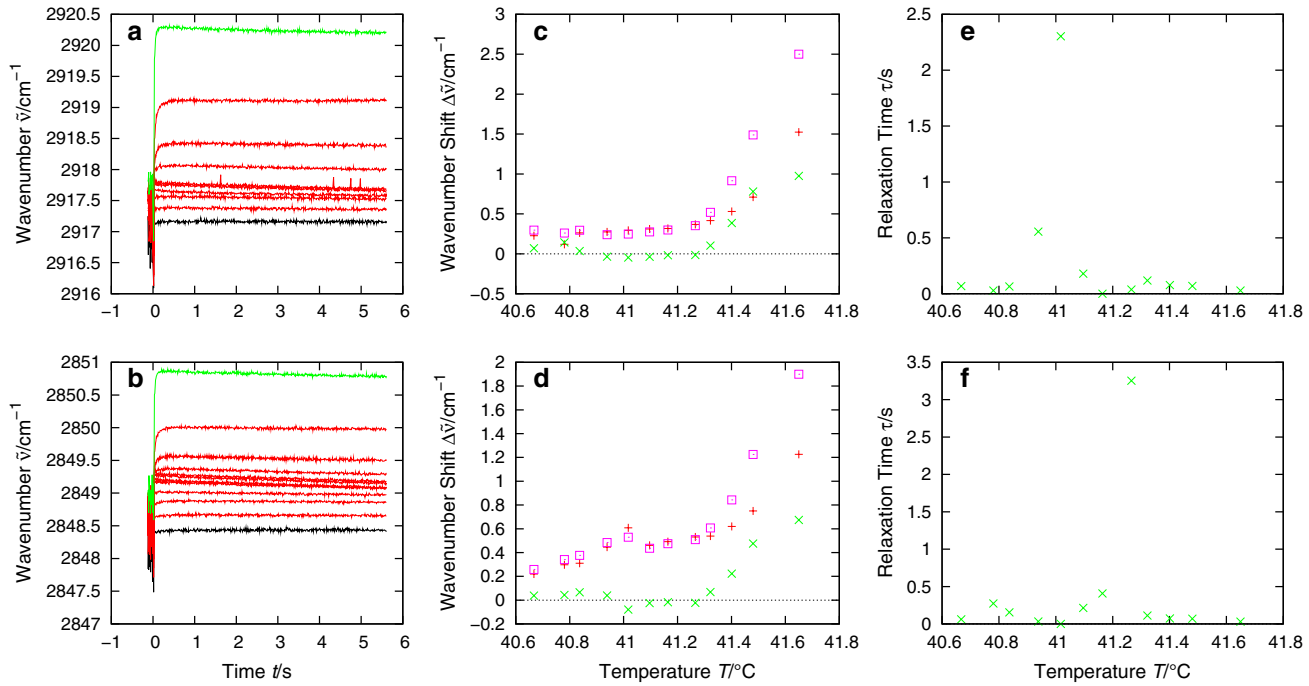

Fig. 4 *Left column* p-jump traces of the $\nu_{as}(CH_2)$ and $\nu_s(CH_2)$ peak (**a**, **b**) of DPPC in a temperature interval from 40.67°C (*black line*) to 41.65°C (*green line*). *Middle column* Amplitudes (**c**, **d**) $\Delta\tilde{\nu}_1$ (*plus*), $\Delta\tilde{\nu}_2$ (*times*), sum of $\Delta\tilde{\nu}_i$ (*square*). *Right column* Relaxation time (**e**, **f**) τ_2 (*times*)

occurs at certain temperatures and is caused by the feed-back loop of the temperature control of the thermostat. This superposition of the decrease in wavenumber leads to problems in the fitting routing giving unacceptable high values for the amplitudes and time constants, which are without any physical background. Therefore, the values for $\Delta\tilde{\nu}_3$ and τ_3 are not shown in Fig. 4. For the same reason, the $\sum\Delta\tilde{\nu}_i$ curve is calculated for $i = 1, 2$ only.

Further experimental difficulties arise from the high cooperativity of the main transition. To achieve a reliable temperature resolution, the temperature fluctuations in the sample volume should be better than the $\approx$0.03 K, which we can achieve with our instrumental setup. For this reason, the results shown are only for purpose of comparison.

The $\sum\Delta\tilde{\nu}_i$ curve in Fig. 4c, d remains almost constant for the first temperature points but then increases sharply at temperatures >41.24°C due to the high cooperativity of the main transition. Maxima of the $\Delta\tilde{\nu}_i$ data are outside of the observed temperature window.

The relaxation constants are in the range of 100 ms. Some values for τ_2 were found in the second range, but because the corresponding amplitudes are very low these values have to be seen with caution.

DMPA

The main transition of phosphatidic acids is generally shifted to higher temperature due to interactions between the headgroups via hydrogen bonds. The transition kinetics were found to be slower as previous measurements with light scattering detection showed. We therefore measured the transition of DMPA at neutral pH (Blume and Hillmann 1986; Elamrani and Blume 1983) to see, whether we could reproduce these effects. Plots of the kinetic $\nu_{as}(CH_2)$, $\nu_s(CH_2)$ and ν(C=O) traces are plotted in Fig. 5a–c. It can be seen that the shape of the curves, especially those which are derived from the methylene stretching vibrations, are very similar. This implies that only small changes in the temperature behavior of the time constants can be expected.

The $\sum\Delta\tilde{\nu}_i$ curves for all vibration modes (Fig. 5d–f) show that the transition is much broader compared to the corresponding curves of DPPC or DSPC. The main changes in spectral parameters appear between 53.43 and 55.13°C. Maximal amplitudes are observed at 54.28°C. The values for the $\Delta\tilde{\nu}_i$ amplitudes are much smaller for the slower processes, i.e. the fast process not resolvable by our experiment has almost 80% of the total amplitude of the process. The $\Delta\tilde{\nu}_i$ data calculated from the ν(C=O) traces have negative values, because the maximum of the C=O band shifts to lower wavenumber in the liquid-crystalline state. Minima in the amplitude can be found at the same temperature at 54.28°C as for the $\Delta\tilde{\nu}_i$ values.

The relaxation constants (Fig. 5g–i) determined are in the 100 ms (τ_2) and 1 s range (τ_3). Well-defined maxima can be found in the temperature dependence of the time

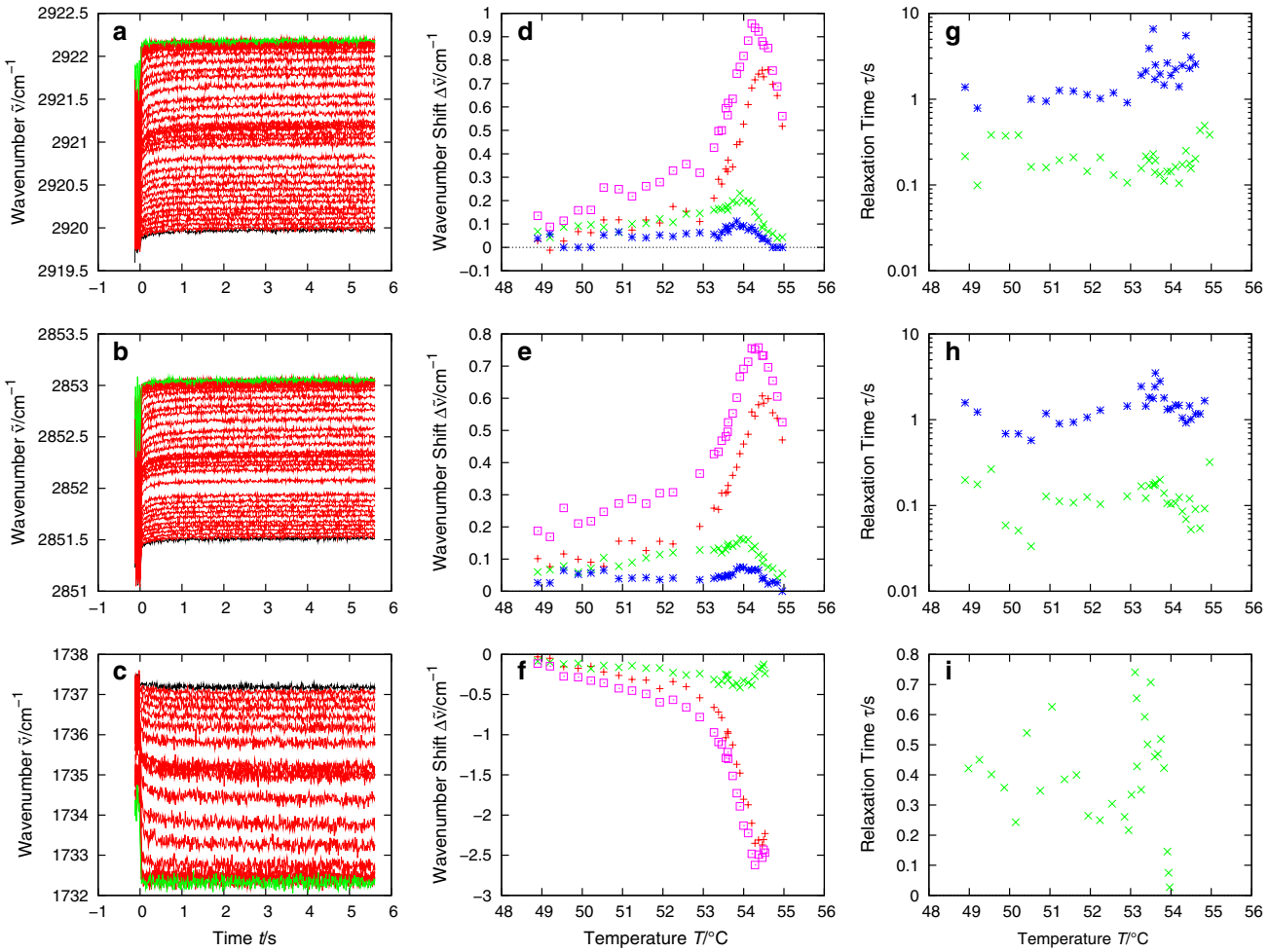

Fig. 5 *Left column* p-jump traces of the $\nu_{as}(CH_2)$ and $\nu_s(CH_2)$ peak (**a**, **b**, **c**) of DMPA in a temperature interval from 48.90°C (*black line*) to 54.61°C (*green line*). *Middle column* Amplitudes (**d**, **e**, **f**) $\Delta\tilde{\nu}_1$ (*plus*), $\Delta\tilde{\nu}_2$ (*times*), $\Delta\tilde{\nu}_3$ (*asterisk*), sum of $\Delta\tilde{\nu}_i$ (*square*). *Right column* Relaxation times (**g**, **h**, **i**) τ_2 (*times*), τ_3 (*asterisk*)

constants derived from the $\nu_s(CH_2)$ traces. They appear at 53.43°C. Curves calculated from the other vibrational bands indicate maxima at the same temperature with comparable values.

DMPE

The kinetic traces and fitting results of the change of the $\nu(CH_2)$ vibrational frequency can be seen in Fig. 6a and Fig. 6b. The curves show, already qualitatively, that a strong temperature dependence of the relaxation constants is present. The amplitude changes are comparable to those observed for DMPA, the corresponding phosphatidic acid having the same acyl chain length. All traces were fitted using a biexponential model. The wavenumber shifts of the ν(C=O) traces are too small compared to the noise level and are therefore not shown in Fig. 6.

Both amplitude curves (Fig. 6a,b) exhibit a maximum at $\approx$50.27°C. Again the slower processes have smaller amplitudes. The temperature dependence of the τ_2 relaxation constant (Fig. 6e,f) shows a peak centered at 49.93°C and its value ranges from 100 ms to 1 s. For this lipid, the maximum in the temperature dependence of the τ_2 values is the most pronounced peak among all lipids investigated in this work.

Discussion

Most investigations of the phase transition kinetics of lamellar lipid phases published so far showed that the kinetics is characterized by multiple processes occurring on different time scales when the the phase transition is induced by an external trigger, such as a T-jump or p-jump. Unfortunately, the detection methods used in these studies were turbidity or fluorescence spectroscopy using labels. These methods are either too unspecific in the case of turbidity or rely on the behavior of a probe molecule,

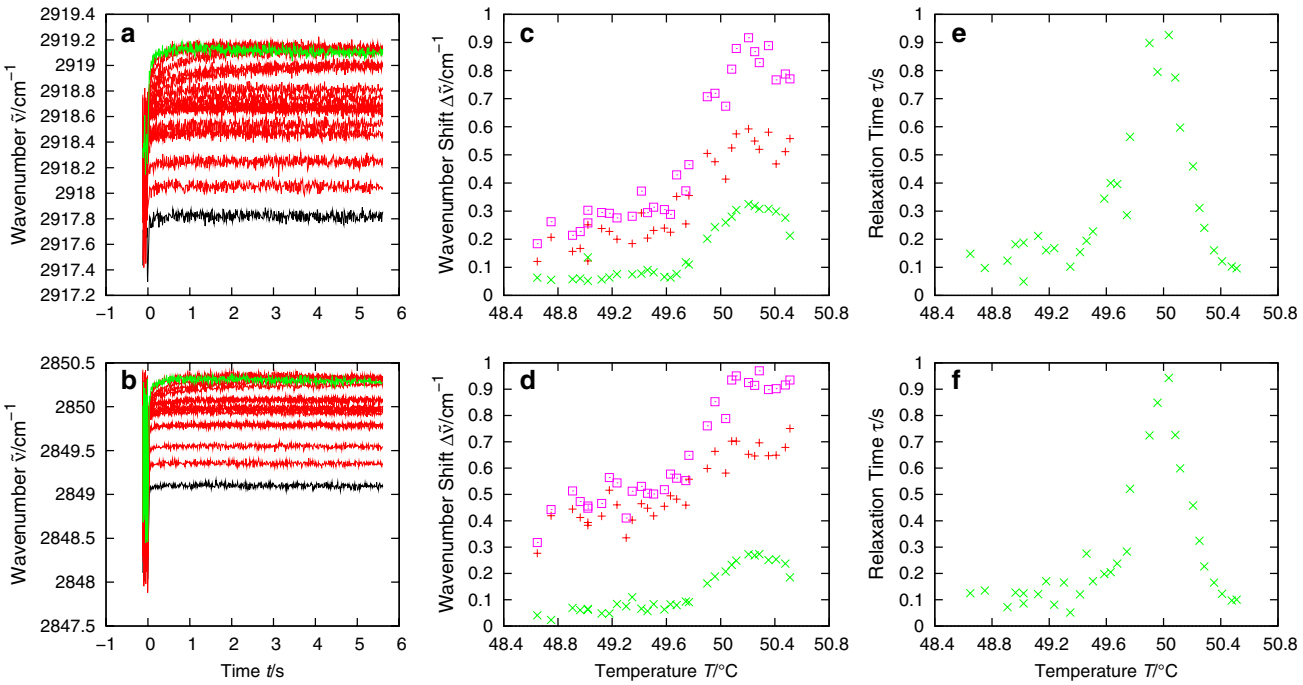

Fig. 6 *Left column* p-jump traces of the $\nu_{as}(CH_2)$ and $\nu_s(CH_2)$ peak (**a**, **b**) of DMPE in a temperature interval from 48.65°C (*black line*) to 50.51°C (*green line*). *Middle column* Amplitudes (**c**, **d**) $\Delta\tilde{\nu}_1$ (*plus*), $\Delta\tilde{\nu}_2$ (*times*), sum of $\Delta\tilde{\nu}_i$ (*square*). *Right column* Relaxation time (**e**, **f**) τ_2 (*times*)

which might not respond in the same way as the lipid molecules themselves. Also, experiments using p-jump calorimetry were reported. However, this method is also unspecific and, in addition, has a very low time resolution so that the fast processes observed here cannot be detected. X-ray scattering methods are in principle very fast. However, the appearance of Bragg-peaks of the new phase depend on cooperative processes of many molecules being arranged in a lattice. Fast conformational changes of individual molecules and processes occurring in an amporphous structure cannot be observed. Moreover, all these methods are sensitive to changes on a macroscopic level only, and not to conformational changes on the molecular level. This was the motivation to develop a p-jump-relaxation method with IR-detection. IR-spectroscopy monitors the vibrational behavior of the individual lipid molecules. This is influenced by the phase state of the lipids. The additional advantage of FTIR-spectroscopy is that in principle different vibrational bands belonging to different moieties in the lipid molecule can be followed. Here, we followed the vibrational bands of the methylene and the C=O groups.

The main result of the p-jump FTIR spectroscopy experiments described above is that the kinetics of the conformational change of the fatty acid chains occurring during the transition from the gel to the liquid-crystalline phase cannot be described by one single process with a defined time constant. Instead, several processes were observed with time constants on different time scales. The results clearly show that the main part of the total amplitude $\sum\Delta\tilde{\nu}_i$ belongs to fast processes that cannot be resolved by the instrument, i.e. have time constants below 8 ms. The remaining processes have smaller amplitudes and, in addition, we could see that the slower the process, the smaller the contribution of the amplitude to the $\sum\Delta\tilde{\nu}_i$. Because, the fast not resolvable processes have the largest amplitude, i.e. shift in frequency of the methylene vibration bands, this implies that the initial conformational change triggered by the p-jump is very fast and probably occurs in individual molecules or small clusters of molecules. This is consistent with the results from turbidity experiments (Elamrani and Blume 1983; Gruenewald et al. 1980), but in contradiction to the recent measurements using p-jump calorimetry (Boehm et al. 2007; Grabitz et al. 2002), where the kinetics of the transition was described by one single relaxation process in the second time regime.

The time dependence of the vibrational frequency was simulated using a model with a fixed number of exponential terms because of the limited signal to noise ratio. However, the shape of the curves indicate that a larger number of exponentials might be more appropriate. The explanation for the complicated transitional behavior is difficult. The occurrence of several relaxation processes is likely an indication that the transition is complex with

possibly fast processes occurring in individual molecules which then form a nucleus of the new phase followed by the formation of larger stable domains which then can grow and coalesce with other domains. Which one of these steps occurs on the fast not resolvable time scale and which one can be attributed to the slowest process in second time regime is unclear. In the model proposed by Kanehisa and Tsong (1978), the nucleation step is the slowest rate determining step and the growth steps are faster. A more detailed model was proposed by Eck and Holzwarth (1984), in which the kinetics proceeds through several steps covering many orders of magnitude in time constants. Our results here partly support this model in that the initial fast processes have time constants below 8 ms.

The kinetic traces of the DPPC sample show an unusual behavior. The fast increase of the wavenumber of the methylene stretching vibrations immediately after the jump is followed by a slow decrease on a second time scale. This effect was only found with the DPPC samples and was not observed in the the kinetic traces of the DSPC, DMPA and DMPE samples. We concluded, therefore, that this slow decrease in wavenumber is probably an artifact that depends on the actual sample temperature and on the cooperativity of the phase transition, because with lipids having a higher transition temperature and lower cooperativity of the transition the effect vanished.

The DMPE sample shows the clearest cooperative transition effects as observed before by turbidity measurements. In contrast to the other lipids, the kinetic traces of this sample (cf. Fig. 6a,b) seems to consist of one resolvable exponential only in addition to the not resolvable fast process. Again, the slow process has a much larger shift in wavenumber. Approximately 70 % of the total shift in wavenumber occurs at shorter times than 8 ms. Therefore, the temperature dependence of the relaxation constant with its maximum value at the transition midpoint can be clearly observed.

The ν(C=O) absorption band was analyzed for the DSPC and DMPA sample only. Due to the higher noise level of these traces, the number of exponential terms was limited to two and, therefore, only one slow relaxation process could be resolved. The findings are similar to those that were derived from the frequency change of the methylene stretching vibrations: The head group hydration is not one process that takes place in the course of the phase transition, but at least two different processes on different time scales are observed. The wavenumber shift of the slower resolvable process is always smaller than those of the faster steps that appear unresolvable using our instrument. The relaxation constant of the slower process shows a maximum at the transition temperature T_M as expected. The values of T_M are equal to those that were derived from the methylene stretching vibrations of the corresponding lipid sample.

Table 1 Relaxation constants at the temperature T_M in comparison with published data

Lipid	τ_2/s	τ_3/s	τ_{max}/s(method)[a]
DSPC	0.1	2.1	30 s (PPC)[b]
DPPC	0.4	–	0.04 s (UV)[c], 30 s (PPC)[b,d]
DMPA	0.08	3.5	0.7 s (UV)[e]
DMPE	0.9	–	–

[a] *UV* turbidity, *PPC* pressure perturbation calorimetry

[b] Boehm et al. (2007)

[c] Gruenewald et al. (1980)

[d] Grabitz et al. (2002)

[e] Elamrani and Blume (1983)

The relaxation constants measured with FTIR spectroscopy at the transition temperature T_M of the corresponding lipid differ from those determined with other techniques (cf. Table 1). The data calculated from the turbidity traces are in the millisecond range and, therefore, faster than ours. In both experiments, the comparable p-jump amplitudes (110 and 150 bar vs. 100 bar) were used, but the jump time used in the turbidity apparatus was ca. two orders of magnitude shorter (60 μs vs. 4 ms). This is the reason why these authors (Elamrani and Blume 1983; Gruenewald et al. 1980) were able to find a larger number of relaxation terms.

The p-jump relaxation constants determined with calorimetry detection are one order of magnitude longer than ours. The instrumental response time is 5 s and the limit of the resolution was estimated to 1–2 s (Grabitz et al. 2002). Therefore, only processes with longer time constants can be observed. This was indeed the case, i.e. for DPPC multilamellar vesicles the maximum relaxation time observed at the transition midpoint was 40 s while for unilamellar vesicles a maximum of 3.2 s was observed. While the setup of Heimburg's group (Grabitz et al. 2002) allows a change of 100 bar during the jump, the jump amplitude of Hinz (Boehm et al. 2007) is limited to 4 bar. Both authors find similar results for DPPC. This is a hint that the amplitude of the p-jump has only little influence on the result. In principle, p-jumps with variable pressure changes could also be performed with our instrument with FTIR detection. However, the change in chain order and thus the change in wavenumber would be correspondingly smaller so that the signal to noise ratio would decrease accordingly. Therefore, we have refrained from performing these experiments. In view of the results by Grabitz et al. and Boehm et al., who obtained similar results with different p-jumps we believe that the amplitude of the p-jump does not influence the kinetics. Rather the end-point after the p-jump determines the kinetics. This is also the consequence of a theoretical description suggested by

Kanehisa and Tsong (1978), where the maximum of the relaxation time is always observed at the transition midpoint at ambient pressure regardless of the starting point.

The results obtained by our new p-jump relaxation technique with IR-detection can thus be summarized as follows: the p-jump experiment with IR-detection clearly shows that major conformational changes in the course of the phase transition from the gel to the liquid-crystalline phase in lipid bilayers occur on time scales below 10 ms not resolvable by our instrument. The transition proceeds in different steps, the one with the longest relaxation times being in the second time range. However, these processes are connected with only small changes in frequency, the major change in order is on a much faster time scale. The results obtained here support the previous findings using p-jump techniques with turbidity detection or fluorescence probes and also favor the model for the transition process presented by Eck and Holzwarth (1984), who proposed a transition model involving a sequence of steps starting from individual molecules to the formation of clusters of the opposite phase and their growth where the steps have different time constants.

Acknowledgments We thank Marina Krumova, Uwe Heuert and Günter Hempel from the Department of Physics of the Martin-Luther-University Halle–Wittenberg for close collaboration. This project was supported by the DFG through the SFB 414, TP 8.

References

Blume A, Hillmann M (1986) Dimyristoylphosphatidic acid cholesterol bilayersthermodynamic properties and kinetics of the phase-transition as studied by the pressure jump relaxation technique. Eur Biophys J 13(6):343–353

Blume A, Hübner W, Messner G (1988) Fourier-transform infrared-spectroscopy of C–13=O-labeled phospholipids hydrogen-bonding to carbonyl groups. Biochemistry 27(21):8239–8249

Boehm K, Guddorf J, Hinz HJ (2007) Application of pressure-modulated differential scanning calorimetry to the determination of relaxation kinetics of multilamellar lipid vesicles. Biophys Chem 126(1–3):218–227

Cameron DG, Kauppinen JK, Moffatt DJ, Mantsch HH (1982) Precision in condensed phase vibrational spectroscopy. Appl Spectrosc 36(3):245–250

Eck V, Holzwarth JF (1984) Fast dynamic phenomena in vesicles of phospholipids during the phase transition. In: Mittal KL, Lindmann B (eds) Surfactants in solution. Plenum Press, NY, pp 2059–2079

Eigen M (1968) Die "unmeßbar" schnellen Reaktionen (Nobel-Vortrag). Angew Chem 80:892–906

Elamrani K, Blume A (1983) Phase-transition kinetics of phosphatidic-acid bilayers a pressure-jump relaxation study. Biochemistry 22(14):3305–3311

Erbes J, Gabke A, Rapp G, Winter R (2000) Kinetics of phase transformations between lyotropic lipid mesophases of different topology: a time-resolved synchrotron X-ray diffraction study using the pressure-jump relaxation technique. Phys Chem Chem Phys 2(1):151–162

Grabitz P, Ivanova VP, Heimburg T (2002) Relaxation kinetics of lipid membranes and its relation to the heat capacity. Biophys J 82(1):299–309

Gruenewald B, Blume A, Watanabe F (1980) Kinetic investigations on the phase-transition of phospholipid-bilayers. Biochim Biophys Acta 597(1):41–52

Kanehisa MI, Tsong TY (1978) Cluster model of lipid phase-transitions with application to passive permeation of molecules and structure relaxations in lipid bilayers. J Am Chem Soc 100(2):424–432

Schiewek M, Krumova M, Hempel G, Blume A (2007) Pressure jump relaxation setup with IR detection and millisecond time resolution. Rev Sci Instrum 78(4):045,101

Winter R, Czeslik C (2000) Pressure effects on the structure of lyotropic lipid mesophases and model biomembrane systems. Z Kristallogr 215(8):454–474